Modeling Surface Runoff Under Climate Change Scenarios: An Integrated SCS-CN and GIS Techniques in a High Andean Basin of Puno, Peru

Calizaya, E.,[1,2*] Aráoz, J.,[1,2] Sardón, S.,[1,2] Calizaya, F.[3] and Laqui, W.[4]
[1]Universidad Nacional del Altiplano, Puno, Perú, Escuela Profesional de Ingeniería Topográfica y Agrimensura (EPITA), E-mail: ecalizaya@unap.edu.pe,* juanaraoz@unap.edu.pe, saulsardon@unap.edu.pe
[2]Instituto de Investigación en Geomática Aplicada, Geotecnologías Espaciales y Terrestres (IGEOMAGET) – EPITA, UNA - Puno, Perú
[3]Universidad Nacional del Altiplano, Escuela Profesional de Ingeniería Agronómica, Puno, Perú
E-mail: fcalizaya@unap.edu.pe
[4]Universidad Nacional del Altiplano, Facultad de Ingeniería Agrícola, Puno, Perú
E-mail: wlaqui@unap.edu.pe
Corresponding Author

DOI: https://doi.org/10.52939/ijg.v21i3.3987

Abstract
Surface runoff is crucial in the hydrological cycle, influencing freshwater availability, soil erosion, and water quality. Climate change will alter precipitation patterns, increasing floods and droughts, exacerbating soil erosion, and affecting the ability of watersheds to retain and filter water, which will impact global water security. This study analyzes surface runoff in the Huancané river basin, Peru, highlighting its importance for water resource management in climate change, using historical precipitation data (1956-2009) from SENAMHI and climate models (HadGEM3-GC31-LL and MPI-ESM1-2-HR) under the ssp126 and ssp585 scenarios. The methodology included using the Curve Number (CN) method for different land covers, soil, and slopes, together with overlapping thematic maps to analyze the spatial variability of runoff. The results show that areas with impermeable soils and open vegetation register the highest runoff values. At present, runoff varies between 0-230 mm (869.3 km²), 230-460 mm (1583.0 km²), and 460-636 mm (1107.8 km²). Under the ssp126 scenario, significant increases in precipitation and runoff are projected, especially in the lower part of the basin, with values that can reach up to 720 mm and affect 1517.8 km². For the ssp585 scenario, runoff values increase even more, with areas experiencing up to 720 mm of runoff affecting 1488.8 km². The weather stations analyzed show significant increases in future precipitation, with an average increase of 100-300 mm, exacerbating runoff problems, particularly in areas with impermeable soils and high slopes. We conclude that integrated watershed management that considers conserving vegetation cover, implementing efficient drainage systems, and sustainable agricultural practices is essential to mitigate the negative impacts of runoff. Long-term planning and collaboration between different stakeholders will be crucial to face the challenges of climate change and protect the natural resources of the Huancané river basin, ensuring its sustainability and resilience.

Keywords: Curve Number, Climate Change Scenarios, Overlapping, Surface Runoff, Spatial Variability

1. Introduction

Earth's most precious resource, water, is recognized as an extraordinary natural resource vital to global socioeconomic progress [1]. A serious risk to water resources is posed by altered terrestrial hydrological processes brought on by climatic patterns and overgrazing changes. These changes have also resulted in soil erosion, decreased water retention, and degraded water quality [2] and [3]. Drinking, farming, producing electricity, and transportation are the four areas of water that humans depend on the most. Because water travels over and through the entire land on Earth's surface, it forms river basins or watersheds [4] and [5]. One of the primary hydrological processes in the catchment, runoff, is influenced by soil layers, surface topography, drainage patterns, and geomorphic units [6]. According to its definition, water moves overland from a saturated soil layer at a specific time[7].

Understanding the hydrological regime and the risks associated with flooding can be done by quantitative runoff estimation [8] and [9].

The researchers experiment with several techniques to identify an appropriate and reliable approach for runoff volume estimation. The Rational and SCS-CN methods are the most popular approaches [10] and [11]. For the past 60 years, the US Department of Agriculture's Soil Conservation Service (SCS) has been using the curve number (*CN*) method to anticipate the flood runoff depth from ungauged catchments [12]. The predicted discharge from the rational approach is unnecessary and more conservative than the initial condition. Due to its affordability, ease of use, and ability to estimate runoff, the SCS-CN approach has gained traction over the Rational method [13]. Hydrologic computer models of physically based catchments that are spatially distributed can be used to calculate the runoff generation sequences for a particular rainfall event [14].

The soil type, moisture content, vegetation cover, topography, and land use all affect the coefficient when rainfall-producing runoff happens [15] and [16]. The GIS is essential in hydrological modeling because it manages vast spatial and attribute data. Its capabilities, including map overlay and analysis, are beneficial for deriving and aggregating hydrological parameters from various sources, such as soil, land cover, and rainfall data [17] and [18]. The percentage of rainfall that turns into direct runoff during an event is known as the runoff coefficient. Event runoff coefficients have been applied in the 20th century [19]. Runoff coefficient can be defined as the maximum rate of runoff to the intensity of the rainfall during the concentrated period, or as the total depth of runoff, to the total depth of rainfall [20][21] and [22]. One of the valuable sources for assessing the impact of climate change on water resources is the Coupled Model Intercomparison Project's (CMIP) global climate models (GCMs), which contain information on how the climate has evolved and are, as a rule, general [23]. Global Climate Models (GCMs) are essential for assessing worldwide climate change impacts [24]. Despite their predictive strength, GCMs face inherent limitations, particularly their low spatial resolution, which can restrict their utility in localized or regional analyses. Therefore, to obtain local scale climate estimates, GCM processing is required [25]. However, there remains a dearth of research on the characterization of surface water runoff under climate change conditions and the variability of water in space.

This study quantified the influences of climate change on surface runoff. Specifically, precipitation (mm) was selected to represent the current surface runoff, and the environmental characteristics in the basin of land cover, soil permeability, and slope were chosen to quantify the impact of the different factors on runoff in the "reference period" (1956-2009) and the "impact period" (2021-2040). In addition, the latest CMIP6 climate model products were used to analyze the scenarios used in the surface water runoff model. The main objectives were: 1) To quantify the current surface runoff using the *CN* method; 2) To determine the spatial variability of surface runoff under hypothetical climate change scenarios; 3) To evaluate and analyze the potential impact of climate change on precipitation concerning environmental variables on surface runoff in 2040.

2. Materials

2.1 Study Area

Figure 1 shows the Huancané River basin is located in the Puno region, in southeastern Peru, in the Andean Altiplano, with approximate geographic coordinates of 15°30' to 15°00' south latitude and 69°30′to 70°00′ west longitude. It covers an area of approximately 3,560 km². The mouth of its main river flows into the highest navigable lake in the world, Lake Titicaca, at 3820 m above sea level, and the maximum elevation of the basin is 5137 m above sea level. This watershed was selected because it is vital to the region's agriculture since it supplies water for the irrigation of crops like barley, quinoa, and potatoes, which are necessary for the population's subsistence and the economy, and is characterized by complex topography, varied land use, and a high dependence on its water resources for agriculture and local livelihoods. Frequent flood events and soil erosion, especially during the rainy season, have been reported in the basin, exacerbated by steep slopes, impermeable soils, and erratic precipitation patterns. Additionally, the basin is increasingly vulnerable to climate change, with projections indicating heightened rainfall intensity and variability, which could amplify runoff, flood risks, and associated impacts on ecosystems and communities. Studying this basin provides valuable insights into managing water resources and mitigating climate-related risks in similar Andean regions, emphasizing the need for sustainable land use and adaptive hydrological practices.

The Huancané River also provides the villages with potable water, essential for their health and welfare. The basin's surface water resources sustain various habitats and are necessary for commercial pursuits like fishing and cattle grazing. This watershed must be appropriately managed to preserve the quantity and quality of water.

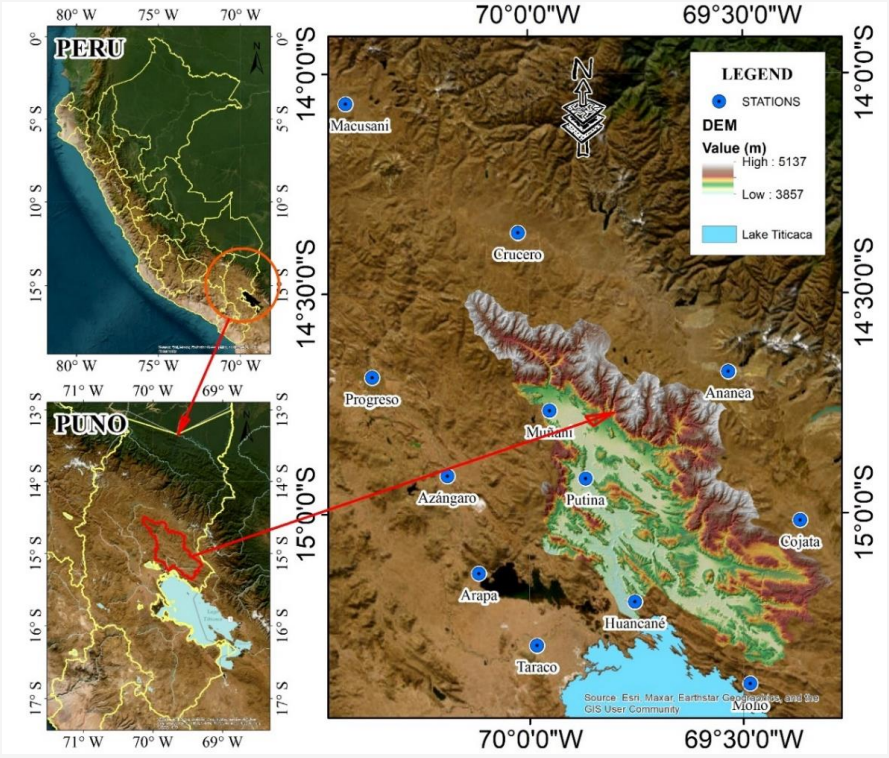

Figure 1: Huancane River basin and the locations of climatological stations

Table 1: Multiannual average precipitation for the period (1956 - 2009) - SENAMHI

Stations	Precipitation (mm)
Ananea	621.7
Muñani	644.4
Putina	693.2
Azángaro	609.4
Progreso	614.5
Crucero	783.5
Macusani	622.7
Cojata	743.6
Huancané	677.7
Arapa	695.8
Moho	885.1
Taraco	591.3

Due to its significant hydrological and environmental challenges, it is an ideal case for analyzing surface runoff dynamics under current and future climatic conditions.

2.2 Dataset and Processing

2.2.1 Climate data

For this study, we utilized precipitation data from two distinct sources and periods, each carefully selected and processed to ensure methodological consistency and robustness; the climatological information on total multiannual precipitation from 1956 to 2009 was used, covering 68 years of historical records Table 1; these data were provided by Autoridad Nacional del Agua and the National Water Authority through the Servicio Nacional de Meteorología e Hidrología (SENAMHI) - Peru. (https://www.senamhi.gob.pe/site/descarga-datos/) These data are crucial for studies like ours, as they are collected from a reliable network of meteorological stations across Peru, ensuring accuracy and relevance for regional climate and hydrological assessments. WorldClim Data (2010–2020): The data from WorldClim for this period represents historical precipitation records that have been processed as multi-annual averages.

These data were utilized to align and compare with the corrected SENAMHI records, facilitating the identification of patterns and trends. The WorldClim dataset provided a critical baseline for bridging potential inconsistencies between observed and modeled datasets. Projected Data (2021–2040); it incorporated downscaled precipitation data based on CMIP6 climate models for future climate projections. These projections, derived from two distinct climate change scenarios, were calibrated and bias-corrected using WorldClim v2.1 as the baseline climate dataset. It ensures the reliability of the predictions, as they are consistent with observed climate variability and trends. The climatological data were analyzed, corrected, and completed using advanced statistical models. This precipitation information generated thematic isohyet maps of the multiannual total for the Huancané river basin. These maps were created using Geographic Information System (GIS) tools and the Inverse Distance Weighting (IDW) interpolation method, facilitating their subsequent geoprocessing and other environmental variables see Figure 2.

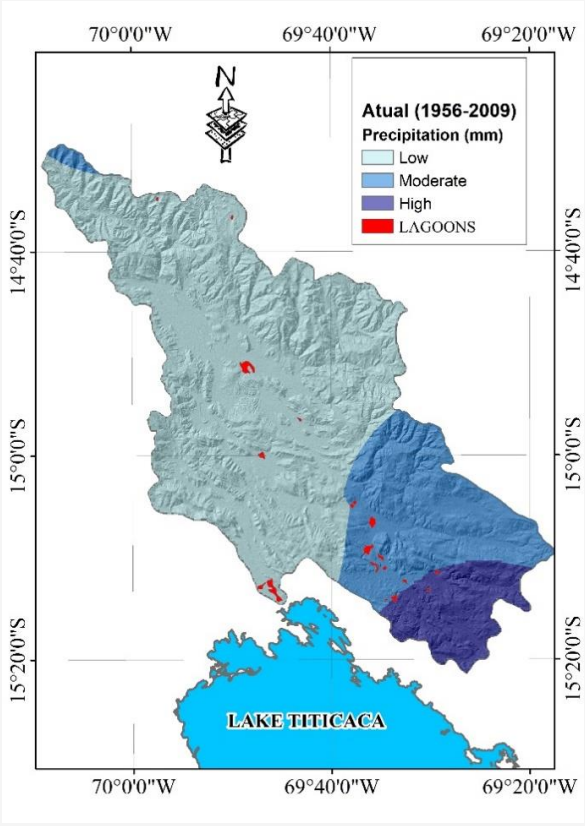

Figure 2: Spatial variability of SENAMHI multiannual average rainfall from 1958 to 2009 using the IDW interpolation method

To ensure the consistency and reliability of the precipitation data, it was conducted a thorough analysis that included visual inspection of hydrographs to identify anomalies, double mass analysis to verify the internal consistency of cumulative precipitation data, and statistical tests such as jump analysis and trend analysis to detect abrupt changes and long-term patterns, respectively. We utilized the HEC-4 Monthly Streamflow Simulation software to address missing data, which applies stochastic modeling to generate consistent monthly streamflow estimates based on precipitation relationships. These robust methods ensured the dataset was complete, reliable, and suitable for hydrological analysis.

3. Methodology

Surface runoff was estimated using the Soil Conservation Service Curve Number (SCS-CN) method [26]. The precipitation variable was vital in this method, as it determines the water available for runoff after initial soil needs, such as infiltration and retention, have been met. In addition, global climatological models HadGEM3-GC31-LL and MPI-ESM1-2-HR, which are considered the most promising for studies in Puno due to their high spatial resolution, were used, two sustainability Taking the Green Road (SSP) scenarios were used to project future changes in surface runoff for this research, the SSP126 scenario that assumes sustainable development and the SSP585 scenario that assumes uncontrolled development without protecting the environment and other factors, Spatial analysis in ArcMap is performed using overlay tools to combine these thematic maps and generate a final *CN* map, it shows in Figure 3. This integrated map allows for the spatially distributed calculation of surface runoff using the *CN* SCS method [27]. These combined approaches allowed us to project the change in surface runoff in the basin to the year 2040, providing a more complete and detailed view of the potential impacts of climate change.

3.1 Method of Runoff Estimation

The Soil Conservation Service Curve Number (SCS-*CN*) method is widely used for estimating surface runoff in watersheds [28] and [29]. This method integrates several environmental factors to calculate runoff, including land cover, slopes, and soil characteristics (permeability or infiltration rate) [30]. The basic Equation 1 and Equation 2 of the SCS-CN method is:

$$Q = \frac{P - I_a}{P - I_a + S}$$

for $P > I_a$, and $Q = 0$ for $P \leq I_a$

Equation 1

Where:

Q is the surface runoff (mm).
P is the total precipitation (mm).
I_a is the initial retention, typically = O.2S (mm)
S is the maximum potential retention after the onset of runoff (mm) and is calculated as:

$$S = \frac{25,400}{CN} - 250$$

Equation 2

Where CN is the Curve Number, a dimensionless value that varies according to land cover, soil type, and moisture conditions.

3.2 Land Cover Map

Classify the different land use and land cover classes, assigning a CN value to each class based on standard SCS tables. LULC is a significant topic element in the study analysis. It details how land is now used and patterned. Remote sensing satellite mapping is commonly employed because LULC is changing quickly. Most natural vegetation types, terraced bare soil, and rocks are included in the Land Use and Land Cover (LULC) technique, which is widely used to estimate the impact of watershed cover on infiltration and runoff. For the investigation, see Figure 4. We utilized the CORINE Land Cover methodology for the Land Use/Land Cover (LULC) classification, which is widely recognized for its structured and consistent approach. The LULC data were derived from a Landsat 7 Enhanced Thematic Mapper Plus (ETM+) satellite image captured in 2011 with a spatial resolution of 30 meters. The classification was conducted at a scale of 1:100,000, ensuring a balance between detail and regional applicability.

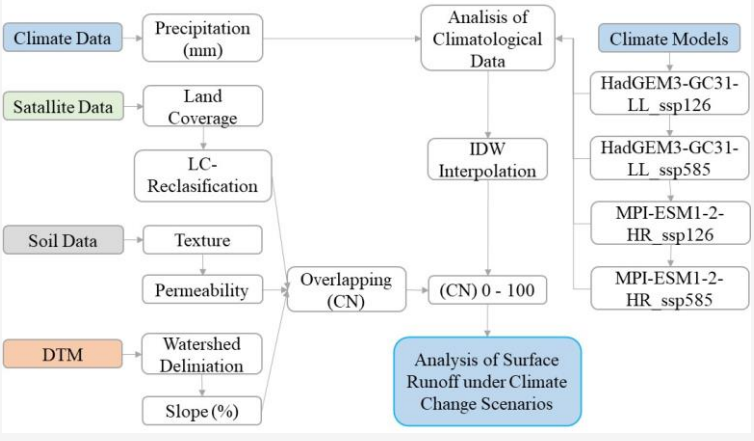

Figure 3: Runoff estimation methods and climate change scenarios

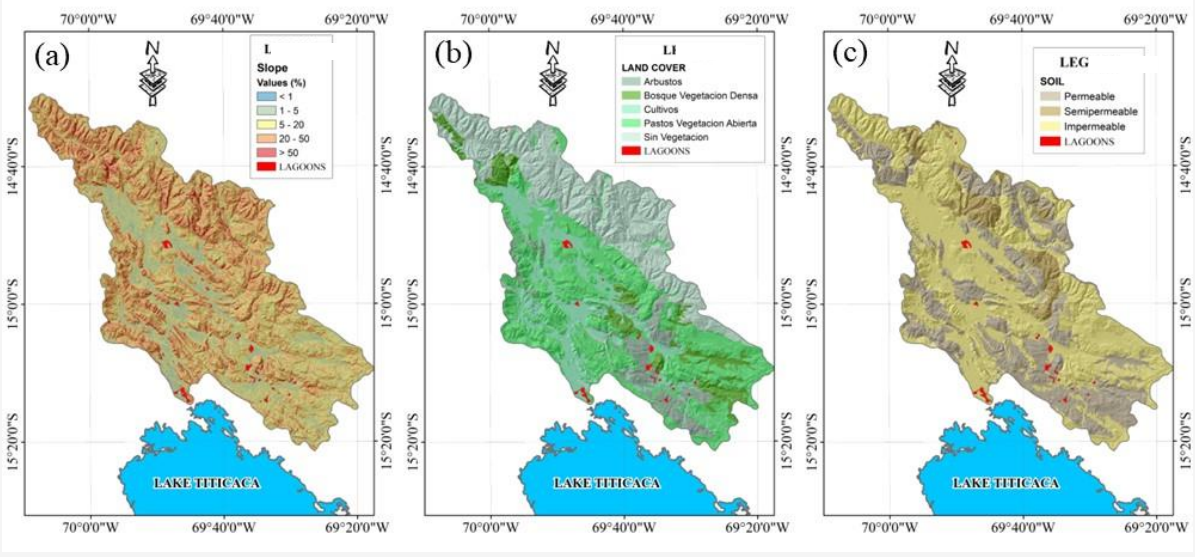

Figure 4: Environmental variables for CN coefficient determination:
(a) slope (b) land cover (c) soil permeability

3.3 Slope Map

For the Digital Terrain Model (DTM), we employed data from the ALOS PALSAR (Advanced Land Observing Satellite – Phased Array type L-band Synthetic Aperture Radar) sensor, with a spatial resolution of 12.5 meters, which provided high precision in representing the terrain. This dataset was particularly useful for hydrological modeling, as its acceptable resolution allowed accurate delineation of the basin and its associated relief features. DTM was used to obtain the slope ranges in percent. Following the recommendations of the Soil Conservation Service (SCS-CN) Curve Number method, these slope ranges were reclassified. This information is of utmost importance in surface runoff modeling since the slope of the terrain is a crucial environmental variable that significantly influences the behavior of surface runoff and water infiltration into the soil [31]. The accuracy of high-resolution DTM allows for a detailed representation of the relief, improving slope analysis accuracy [32]. Steeper slopes accelerate surface runoff, reducing infiltration time and increasing erosion risk. On the other hand, gentler slopes favor infiltration and reduce surface runoff [33]. The reclassification of slope ranges according to the SCS-CN method facilitates the integration of this variable in hydrological models, allowing a more robust and accurate analysis of surface runoff dynamics in the Huancané river basin, as shown in Figure 4. This methodology is essential for water resources planning and management, especially in mountainous regions with marked topographic variations, and can significantly impact hydrological patterns.

3.4 Soil Type Map

Determination of soil characteristics, such as permeability and infiltration capacity, to adjust the *CN* values. Soil texture is a fundamental characteristic that refers to the relative proportion of different particle sizes of sand, silt, and clay and is essential for estimating the infiltration capacity and permeability of the soil [34]. It is vital in the SCS-CN method, where soil texture helps to define soil classes and assign appropriate *CN* values of permeability Figure 4. We followed a systematic procedure based on the SCS-CN methodology to determine the *CN* values, ensuring accuracy and consistency throughout the analysis. The process involved three key thematic maps: land use/land cover (LULC), soil texture, and slope, which were reclassified according to the criteria specified in Table 2 of the SCS-CN method.

The LULC map was derived from reclassifying the land use categories into SCS-CN-defined groups based on Table 2. Each category was assigned a specific land cover condition, influencing its *CN* value. Soil Texture Map was reclassified to define *permeable*, impermeable, and semipermeable categories. These classifications were aligned with the hydrological soil groups outlined in the SCS-CN methodology, representing varying infiltration capacities. The slope map was reclassified into ranges of inclination, as defined in Table 2, to reflect the impact of slope steepness on runoff potential. Steeper slopes were associated with higher runoff coefficients, while gentler slopes corresponded to lower values.

Table 2: Methodology to determine the *CN* coefficient by overlaying three environmental variables: land cover, soil permeability, and slope

Land Cover	**Soil Type**	**Slope (%)**				
		< 1	**1 - 5**	**5 - 20**	**20 - 50**	**> 50**
No vegetation	Permeable	0.3	0.4	0.4	0.4	0.5
No vegetation	Impermeable	0.6	0.6	0.7	0.8	0.8
No vegetation	Semipermeable	0.5	0.6	0.6	0.6	0.7
Crops	Permeable	0.2	0.3	0.3	0.4	0.4
Crops	Impermeable	0.5	0.6	0.6	0.6	0.7
Crops	Semipermeable	0.4	0.4	0.5	0.6	0.6
Pasture open vegetation	Permeable	0.2	0.2	0.2	0.3	0.4
Open pasture vegetation	Impermeable	0.4	0.5	0.6	0.6	0.6
Pasture open vegetation	Semipermeable	0.4	0.4	0.4	0.5	0.6
Shrubs	Permeable	0.1	0.2	0.2	0.2	0.3
Shrubs	Impermeable	0.4	0.4	0.5	0.6	0.6
Shrubs	Semipermeable	0.3	0.4	0.4	0.4	0.5
Dense forest vegetation	Permeable	0	0.1	0.2	0.2	0.2
Low, dense vegetation forest	Impermeable	0.4	0.4	0.4	0.5	0.6
Moderate dense vegetation forest	Semipermeable	0.2	0.3	0.4	0.4	0.4

Table 3: Precipitation of two global climate models and two climate change scenarios

Stations	HadGEM3-GC31-LL_ssp126	HadGEM3-GC31-LL_ssp585	MPI-ESM1-2-HR_ssp126	MPI-ESM1-2-HR_ssp585
Ananea	899	879	931	931
Muñani	713	698	754	749
Putina	699	689	744	741
Azángaro	744	722	775	770
Progreso	745	736	797	792
Crucero	682	674	732	725
Macusani	685	683	742	736
Cojata	673	664	721	716
Huancané	706	690	752	747
Arapa	800	776	828	822
Moho	855	835	895	894
Taraco	875	861	940	934

Finally, we used GIS tools, and these thematic maps were overlaid to create a combined dataset. The attributes of each layer were manipulated and integrated with the database to assign Curve Number (*CN*) values to each unique combination of land use, soil texture, and slope.

3.5 Climate Data Scenarios

The model surface water runoff in the Huancané river basin under climate change scenarios shown in Table 3, the HadGEM3-GC31-LL and MPI-ESM1-2-HR global climate change models were used; these models were chosen because of their high resolution and accuracy in representing extreme climate phenomena, In addition to the SSP1 (sustainable development) and SSP5 (fossil fuel driven development) scenarios, both HadGEM3-GC31-LL and MPI-ESM1-2-HR are suitable for studies in the high Andean zone and have the ability to represent the ENSO El Niño phenomenon, which makes them especially useful for climate analysis in this region where ENSO plays an essential role in climate variability. The projected climate data include precipitation and mean annual temperature variables obtained from the WorldClim for 2021 to 2040 [35]. These results will be analyzed and compared to assess the impacts of climate change on the surface runoff of the Huancané River today and with the scenarios applied to 2040, providing crucial information for planning mitigation and adaptation strategies [36].

3.6 IDW Interpolation

This study uses ArcMap software to evaluate multi-year precipitation data from climate change models using the IDW interpolation method. IDW is a deterministic spatial interpolation method where the estimated values are obtained as the average of the known point values within a certain chosen neighborhood, in which the nearest points exert the greatest influence [37]. This method is beneficial for the environmental data, resulting in fairly uniform precipitation distribution over the entire area of research [38]. We examined precipitation data obtained from climate models for the ssp126 and ssp585 scenarios, with years ranging from 2021 to 2040 and historical precipitation data obtained from SENAMHI, which ranged from 1956 to 2009. L=pd1 MPI-ESM1-2-HR, pd2 HadGEM3-GC31-LL. The IDW approach was chosen as more accurate and less complex regarding spatial variability [39].

4. Results

4.1 Modeling of the CN.

The current research adopted the curve number (*CN*) method to estimate the future likely runoff in the Huancané River basin. This region is usually marked by the variation in vegetation cover and the ground's permeability levels. The results revealed a differentiated *CN* value distribution depending on land cover and permeability areas. It does this by raising awareness of the principles of water conservation, proper management of water resources in this specific watershed region, and soil conservation. Published *CN* values for areas with shrub cover and permeable soil types differed significantly from *CN* values determined from our study. Specifically, on slopes less than 1%, we observed a *CN* value of 10, covering an area of 2.9 km². As the slope increases to 1-5%, the *CN* increases to 30, covering an area of 22.7 km². On slopes between 5-20%, the *CN* is reduced to 15, corresponding to a significant area of 144.8 km². However, on 20-50% slopes, the *CN* increases again to 25, covering 97.1 km²; on slopes greater than 50%, the *CN* is 20, covering 4.5 km².

In areas with shrubs and semipermeable soils, the *CN* values are higher, reaching 50 on slopes of 1-5% (0.5 km²) and 45 on slopes of 20-50% (3.6 km²). Areas with dense forest vegetation and permeable soils have the lowest *CN* values, indicating higher infiltration and lower surface runoff. On slopes less than 1%, the *CN* is 5, covering 1.3 km², while on slopes of 1-5%, the *CN* is 25, covering 11.1 km². On slopes of 5-20%, the *CN* is reduced to 10, corresponding to a wide area of 79.6 km², and on slopes of 20-50%, the *CN* is 20, covering 77.2 km². On slopes greater than 50%, the *CN* is 15, covering 11.8 km². When soils are impermeable, *CN* values increase, reaching 55 on slopes of 1-5% (6.6 km²) and 50 on slopes of 20-50% (47.2 km²) see Table 4.

Table 4 shows the areas dedicated to crops with impermeable soils with the highest *CN* values, indicating high runoff and a higher erosion risk. On slopes less than 1%, the *CN* is 50, covering an area of 21.6 km². On slopes of 1-5%, the *CN* reaches 70, covering 136.9 km², while on slopes of 5-20%, the *CN* is 55, covering an extensive area of 250.3 km². On 20-50% slopes, the NC increases to 65, covering 91.7 km²; on slopes greater than 50%, the *CN* is 60, covering 10.5 km². Crop areas with permeable soils present lower *CN* values, with a *CN* of 20 on slopes less than 1% and a *CN* of 35 on slopes of 20-50% (17.9 km²). Pasture areas with open vegetation and impermeable soils also show high *CN* values, reflecting high runoff.

Table 4: Modeling results for determining the *CN* coefficient by the overlapping method

Land Cover	Permeability	Range	*CN*	Area (Km2)	Land Cover	Permeability	Range	*CN*	Area (Km²)
Shrubs	Permeable	< 1%	10	2.9	Pasture Open Vegetation	Impermeable	< 1%	45	10.8
		1 - 5%	30	22.7			1 - 5%	65	80.2
		5 - 20%	15	144.8			5 - 20%	50	425.5
		20 - 50%	25	97.1			20 - 50%	60	329.9
		> 50%	20	4.5			> 50%	55	25.8
	Semipermeable	< 1%	30	0.1		Permeable	< 1%	15	2.7
		1 - 5%	50	0.5			1 - 5%	35	23.5
		5 - 20%	35	4.1			5 - 20%	20	180.1
		20 - 50%	45	3.6			20 - 50%	30	212.5
		> 50%	40	0.4			> 50%	25	19.2
Forest Dense Vegetation	Impermeable	< 1%	35	0.9		Semipermeable	< 1%	35	0.1
		1 - 5%	55	6.6			1 - 5%	55	1.2
		5 - 20%	40	46.4			5 - 20%	40	16.1
		20 - 50%	50	47.2			20 - 50%	50	23.1
		> 50%	45	2.3			> 50%	45	1.0
	Permeable	< 1%	5	1.3	No Vegetation	Impermeable	< 1%	60	2.0
		1 - 5%	25	11.1			1 - 5%	80	18.6
		5 - 20%	10	79.6			5 - 20%	65	221.0
		20 - 50%	20	77.2			20 - 50%	75	345.1
		> 50%	15	11.8			> 50%	70	44.7
Crops	Impermeable	< 1%	50	21.6		Permeable	< 1%	30	0.3
		1 - 5%	70	136.9			1 - 5%	50	4.0
		5 - 20%	55	250.3			5 - 20%	35	76.8
		20 - 50%	65	91.7			20 - 50%	45	153.2
		> 50%	60	10.5			> 50%	40	24.2
	Permeable	< 1%	20	0.0		Semipermeable	< 1%	50	0.3
		1 - 5%	40	0.5			1 - 5%	70	3.0
		5 - 20%	25	7.1			5 - 20%	55	51.5
		20 - 50%	35	17.9			20 - 50%	65	122.0
		> 50%	30	1.1			> 50%	60	19.4

On slopes less than 1%, the *CN* is 45, covering 10.8 km², while on slopes of 1-5%, the *CN* is 65, covering 80.2 km². On slopes of 5-20%, the *CN* is 50, covering an extensive area of 425.5 km², and on slopes of 20-50%, the *CN* is 60, covering 329.9 km². On slopes greater than 50%, the *CN* is 55, covering 25.8 km². In pasture areas with permeable soils, the *CN* values are lower, with a *CN* of 15 on slopes less than 1% (2.7 km²) and a *CN* of 30 on slopes of 20-50% (212.5 km²).

Areas without vegetation, especially impermeable and semipermeable soils, have the highest *CN* values, indicating high runoff and erosion risks. On impermeable soils and slopes less than 1%, the NC is 60, covering 2.0 km², while on slopes of 1-5%, the *CN* reaches 80, covering 18.6 km². On slopes of 5-20%, the *CN* is 65, covering 221.0 km²; on slopes of 20-50%, the *CN* is 75, covering 345.1 km². On slopes greater than 50%, the *CN* is 70, covering 44.7 km². In permeable soils, the *CN* values are lower, with a *CN* of 30 on slopes less than 1% (0.3 km²) and a *CN* of 45 on slopes of 20-50% (153.2 km²). The classification of the Huancané River basin according to the *CN* range shows that most of the basin is in the high-risk category (*CN* between 53-80), covering 2101.1 km² in the lower part of the basin. Low-risk areas (*CN* between 0-26) correspond to 675.1 km², located in the upper part of the watershed, while moderate-risk areas (*CN* between 26-53) cover 784.2 km² in the middle part of the watershed.

4.2 Actual Precipitation and Climate Change Scenarios

The analysis of multi-year precipitation at the 12 SENAMHI meteorological stations, together with projections under the ssp126 and ssp585 climate change scenarios using the HadGEM3-GC31-LL and MPI-ESM1-2-HR models, Figure 5, shows significant changes that pose substantial challenges for water resource management in the Huancané river basin. Historically, average annual precipitation for 1956-2009 ranged from 591.3 mm at Taraco to 885.1 mm at Moho. Comparing these data with projections for 2021-2040, substantial increases are observed at almost all stations. Ananea, for example, could experience an increase of up to 309 mm under the ssp585 scenario with HadGEM3-GC31-LL, while Azángaro and Progreso could see increases of between 130 and 180 mm. Increases in precipitation will directly impact surface runoff, which varies according to land cover and permeability. In the upper part of the watershed, with a low *CN* classification of 0-26 and an area of 2077.6 km², increases in precipitation will intensify runoff on predominantly permeable soils covered by shrubs and dense vegetation. In these areas, *CN* values vary, for example, between 10 for permeable soils with less than 1% vegetation cover and 50 for semipermeable soils with 20-50% cover. It increases the risk of soil erosion and landslides due to more surface water that cannot be efficiently absorbed.

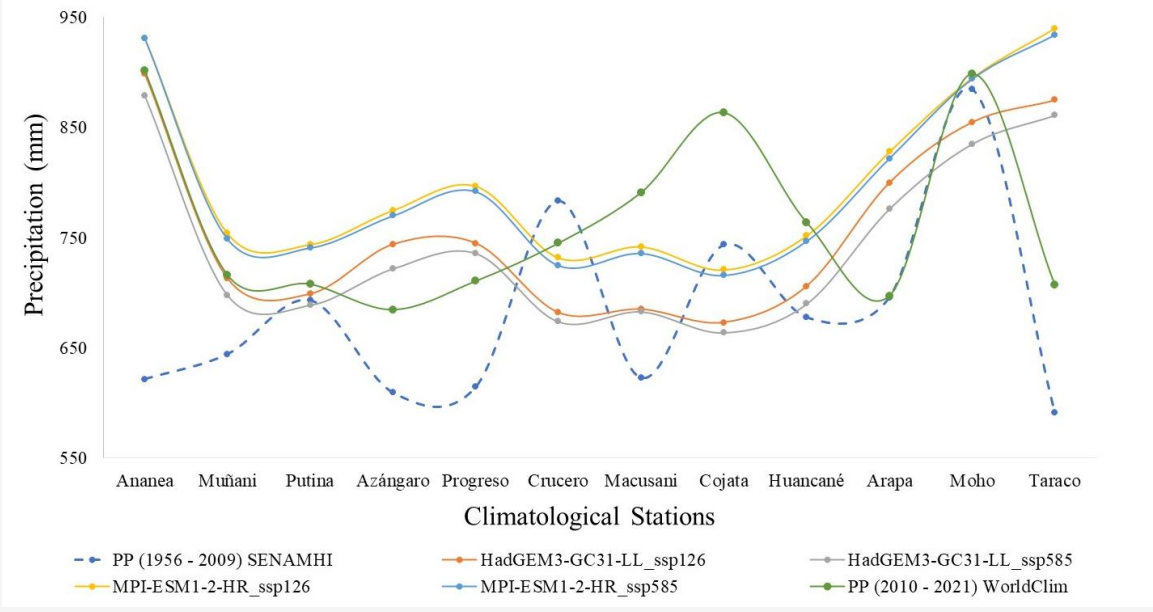

Figure 5: Multiannual average precipitation variation among climate change scenarios

In the middle part of the watershed, with a moderate *CN* of 26-53 and an area of 369.8 km², stations such as Azángaro and Macusani will experience increases in runoff. Land cover in these areas includes open and impervious grasslands with *CN* values ranging from 45 in areas with less than 1% cover to 65 in areas with 1-5% cover. This increase in runoff could saturate soils, increasing the risk of flooding and further eroding the region's water resources. In the lower part of the watershed, with a high *CN* of 53-80 and an area of 1113.0 km², stations such as Taraco and Moho project significant increases in precipitation, resulting in increased surface runoff. This region's soil is predominantly impervious and used extensively for crops, with *CN* values ranging from 50 for impervious soils with less than 1% vegetative cover to 70 in areas with 1-5% cover. It will increase the risk of flooding and compromise water resources' sustainability due to the limited recharge capacity of aquifers in these areas. Figure 6 shows the spatial variability of precipitation in climate change scenarios using the IDW interpolation method.

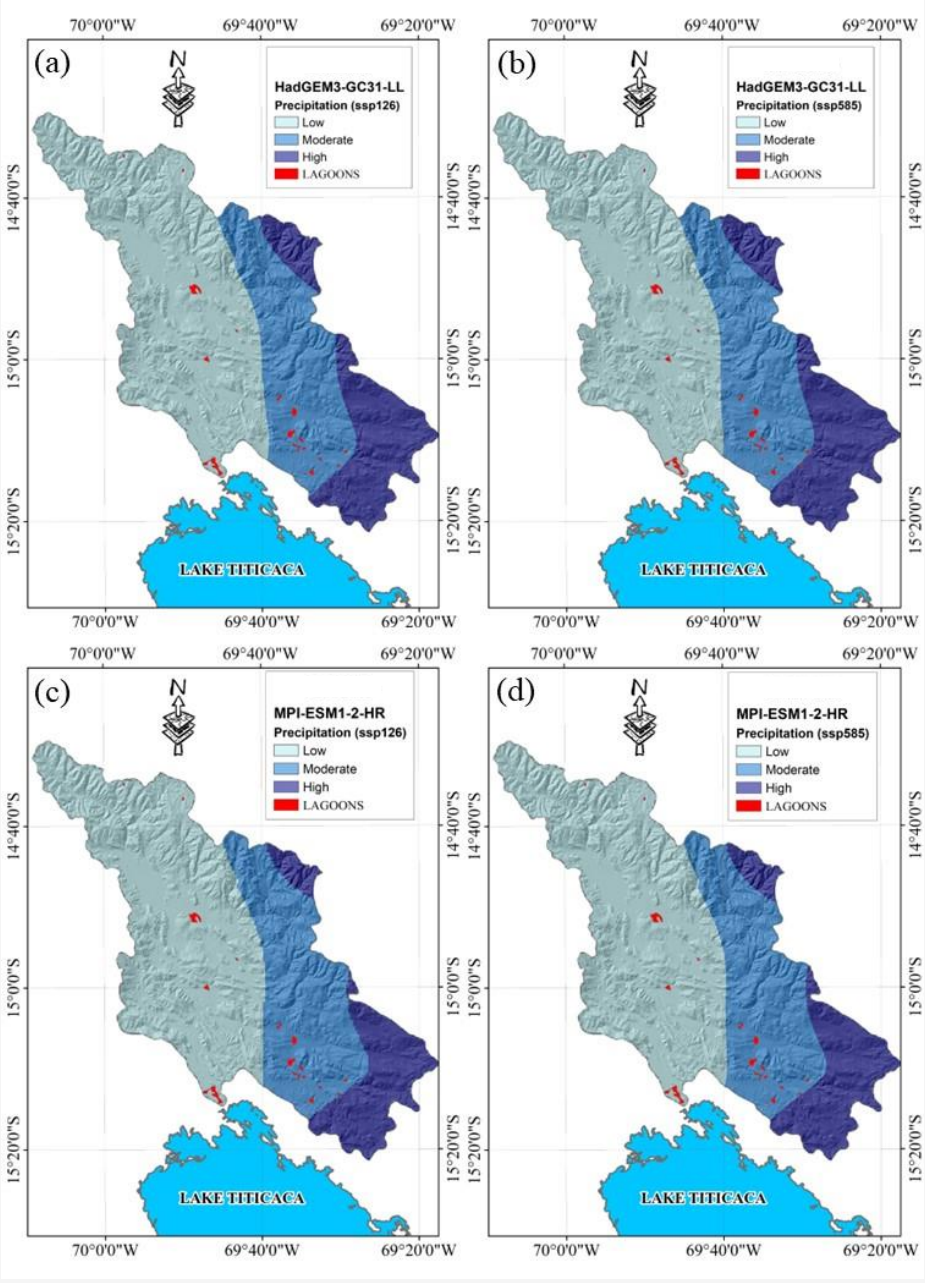

Figure 6: Spatial variability of precipitation of climate change scenarios (a) HadGEM3-GC31-LL - ssp126 (b) HadGEM3-GC31-LL - ssp585 (c) MPI-ESM1-2-HR - ssp126 (d) MPI-ESM1-2-HR - ssp585

Table 5: Results of precipitation and surface runoff between the altitude ranges of the upper, middle, and lower watersheds

Classification (CN)	Range (CN)	Precipitation (mm)	Basin relief (pp)	Runoff (mm)	Basin relief (Runoff)
Low	< 26	630- 711	Upper	< 230	Lower
Moderate	26 - 53	711 - 793	Middle	230 - 460	Middle
High	53 - 80	793 - 875	Lower	460 - 636	Upper

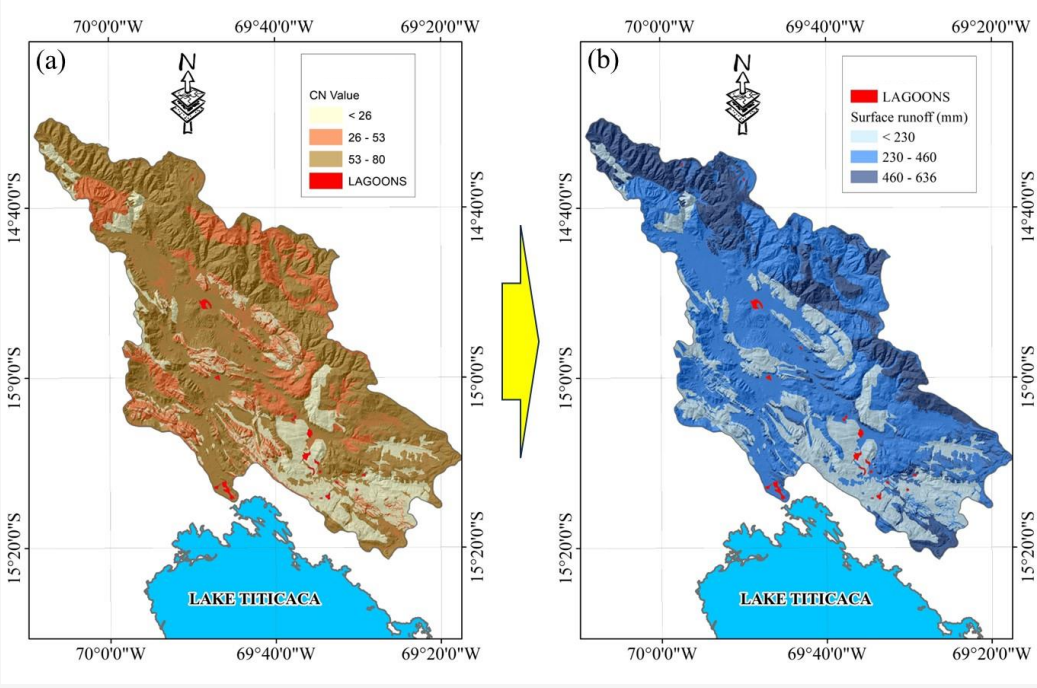

Figure 7: (a) Curve Number values (b) spatial variability of surface runoff

4.3 Modeling of Surface Water Runoff

In this research, improvement was made to the Curve Number (*CN*), with the help of which the runoff in the Huancané River basin was assessed, and a precipitation analysis was completed. Table 5 indicates that overlapping the *CN* values with the precipitation map makes it possible to describe the runoff process in various basin parts with considerably higher accuracy. Figure 7 presents the outcomes that reveal spatial distributions of *CN* values and precipitation significant for decision-making, planning, and conservation of surface water resources. The curve number (*CN*) varies depending on the type of surface cover and the soil infiltration capacity of slopes, representing the runoff capacity. Thus, in the upper part of the basin, the average annual precipitation is 630-711 mm, and the area of land use is 2077. The main airport's six square kilometers comprises permeable and semipermeable land surfaces covered with shrubs and other compact plant growth. In this area, the *CN* values are relatively low, which means there is a significant ability for water infiltration and small surface runoff. The recommendation is that the upper part be a recharge zone, which will help correctly utilize water in the watershed.

This part's third type of climate is characterized by average precipitation of 711-793 mm and occupies 369 square kilometers of the basin. Eight sq km, there is a more significant variation in permeability and vegetation cover of the soils in the area. *CN* values are generally moderate in the soils, which have a semipermeable nature and a mild extent of pasture and shrublands. It is characterized by particular difficulties in runoff management and soil conservation, and special efforts are needed to combat erosion and enhance infiltration. It lies at the lower part of the watershed, with rainfall of 793-875 mm and a land area of 1113 square kilometers. It stands at 0 km², is characterized by a highly impermeable sub-surface, and overlaps vegetation cover with crops. Here, *CN* values are higher to represent higher surface runoff and a higher chance of erosion.

The large area receives high rainfall and has highly impermeable soils that lead to high runoff and much water from the surface; thus, soil conservation and flood control are significant problems. There is a need to incorporate sustainable agricultural practices and enhance the soil structure; this will help control runoff and manage soil erosion in this watershed area.

To achieve the goal of conservation and sustainability, it is relevant to analyze the stability of *CN* values and precipitation in the river basins. There is a need for differential management of the upper, middle, and lower parts of the basin. In the upper part, the measures should protect the potential recharge areas, protect and extend the natural vegetation, and rehabilitate degraded soils. Mix in use; there is a need to implement proper watershed management practices that may include reducing erosion and enhancing infiltration rates. Check dams, agricultural terraces, and conservation agriculture measures, which have to be urgently implemented, are needed in the lower part to control the runoff and minimize the erosion of the depleted soil. These results signify the need to adopt management practices within a basin's watershed that factor in the properties of *CN* values and precipitation of basins. It is essential in enhancing monolith sustainability, increasing soil erosion control, and protecting water resources in the Huancané river basin.

4.4 Surface Runoff Under Climate Change Scenarios

The analysis of current and future surface runoff in the Huancané river basin, considering the ssp126 and ssp585 climate scenarios and the HadGEM3-GC31-LL and MPI-ESM1-2-HR models, reveals significant changes in runoff distribution due to projected increases in multiannual average precipitation (2021-2040). Low runoff (0-230 mm) currently covers 869.3 km², mainly in the upper part of the watershed, characterized by shrub vegetation and dense forest with predominantly permeable soils and low *CN* values (10-25). Areas with moderate (230-460 mm) and high (460-636 mm) runoff cover 1583.0 km² and 1107.8 km², respectively, predominantly in the middle and lower parts of the watershed, where land cover includes crops and open grasslands with impermeable soils and high *CN* values (50-75).

Figure 8 and Table 6 show the ssp126 scenario, which represents a moderate mitigation pathway; notable changes in runoff distribution are observed. Under HadGEM3-GC31-LL, areas with low and moderate runoff are reduced to 869.3 km² and 1583.0 km², respectively, while areas with high runoff increase to 1107.8 km². Figure 9 shows under scenario MPI-ESM1-2-HR, low and moderate runoff decreases to 736.8 km² and 1305.5 km², respectively, and high runoff increases to 1517.8 km². These changes indicate that, under a moderate mitigation scenario, there will be a greater concentration of runoff in the lower and middle parts of the watershed, increasing the risk of soil erosion and landslides in soils with high permeability and dense vegetation cover. The spatial variability results shown in Figure 8, the ssp585 scenario, which represents a high emissions pathway, shows more pronounced changes.

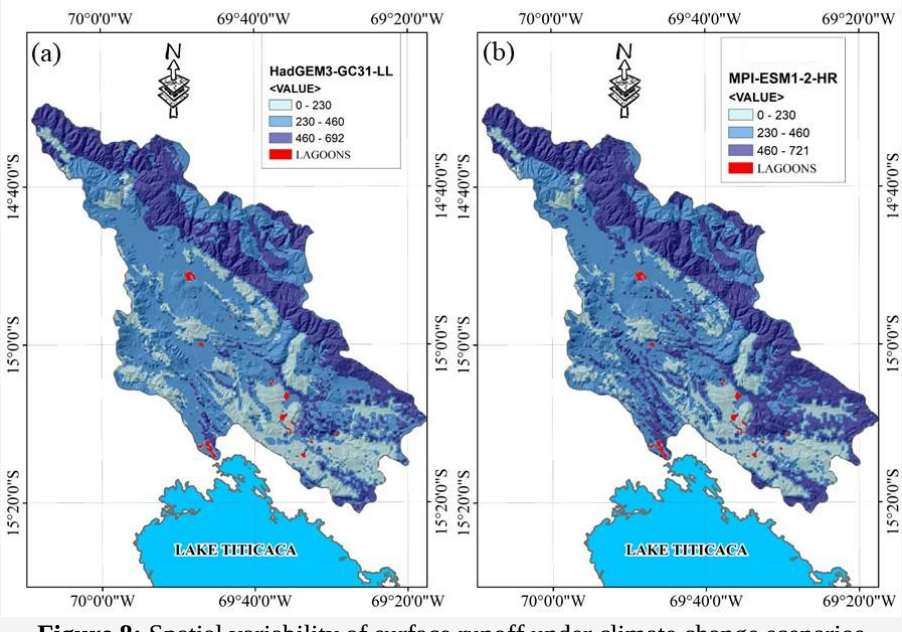

Figure 8: Spatial variability of surface runoff under climate change scenarios (a) HadGEM3-GC31-LL ssp126 (b) MPI-ESM1-2-HR - ssp126

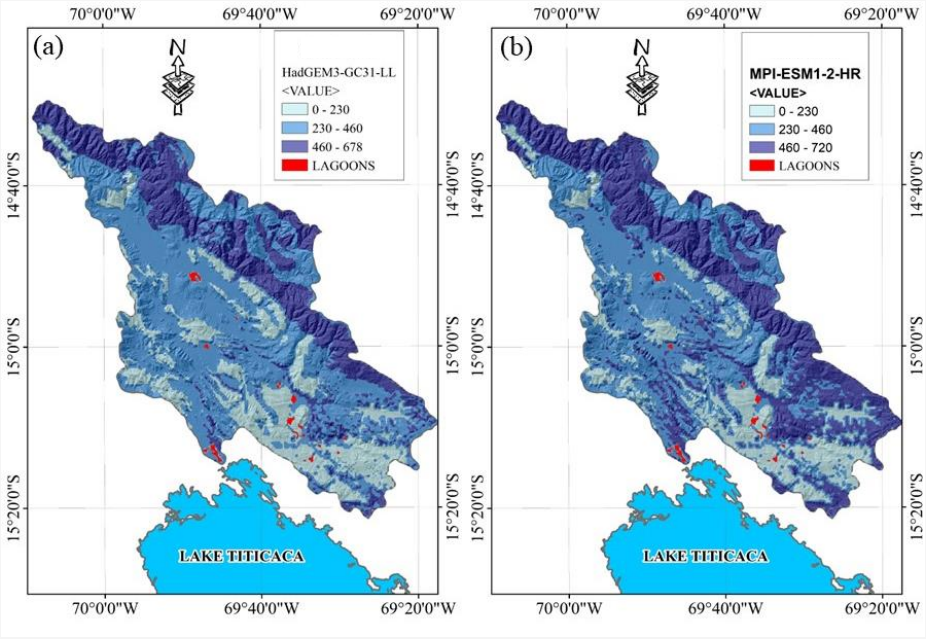

Figure 9: Spatial variability of surface runoff under climate change scenarios (a) HadGEM3-GC31-LL - ssp585 (b) MPI-ESM1-2-HR ssp585

Table 6: Spatial variation of current surface runoff about climate change scenarios concerning their areas in (km^2)

Classification	Actual Runoff (mm)	ssp126				ssp585			
		HadGEM3-GC31-LL		MPI-ESM1-2-HR		HadGEM3-GC31-LL		MPI-ESM1-2-HR	
		Runoff (mm)	Area (Km^2)	Runoff (mm)	Area (Km^2)	Runoff (mm)	Area (Km^2)	Runoff (mm)	Area (Km^2)
Low	0 - 230	0 - 230	869.3	0 - 230	736.8	0 - 230	886.5	0 - 230	749.5
Moderate	230 - 460	230 - 460	1,583.0	230 - 460	1,305.5	230 - 460	1,644.3	230 - 460	1,321.8
High	460 - 636	460 - 692	1,107.8	460 - 721	1,517.8	460 - 678	1,029.3	460 - 720	1,488.8

Under HadGEM3-GC31-LL, areas with low and moderate runoff are reduced to 886.5 km² and 1644.3 km², respectively, while areas with high runoff increase to 1029.3 km² Table 6. Figure 9 shows the MPI-ESM1-2-HR projects a similar reduction in low and moderate runoff areas to 749.5 km² and 1321.8 km², respectively, and an increase in high runoff areas to 1488.8 km². These projections suggest that under a high emissions scenario, the basin will experience a considerable increase in surface runoff, especially in the lower and middle parts, where soils are more impermeable, and land cover includes extensive cropland and open grassland areas. The ssp126 and ssp585 climate change scenarios predict an increase in areas with high surface runoff (460-636 mm) in the Huancané river basin. Under ssp126, the affected area varies between 1107.8 km² with HadGEM3-GC31-LL and 1517.8 km² with MPI-ESM1-2-HR, while under ssp585, the affected areas are 1029.3 km² and 1488.8 km² respectively.

These projections highlight the urgent need for sustainable management and climate change adaptation strategies to mitigate adverse effects on water resources and soil stability.

These results pose several challenges for conserving water resources in the Huancané River basin. Increased surface runoff in areas with impermeable soils and high *CN* values can aggravate soil erosion and increase the risk of flooding. The loss of native vegetation in the upper parts of the watershed, which is crucial for water recharge, and the expansion of crops in areas vulnerable to erosion are problems to be addressed. Implementing sustainable watershed management practices, such as constructing agricultural terraces, installing check dams, and adopting conservation agriculture techniques, is imperative. These measures will help control runoff, protect the soil, and ensure the long-term sustainability of water resources in the Huancané river basin.

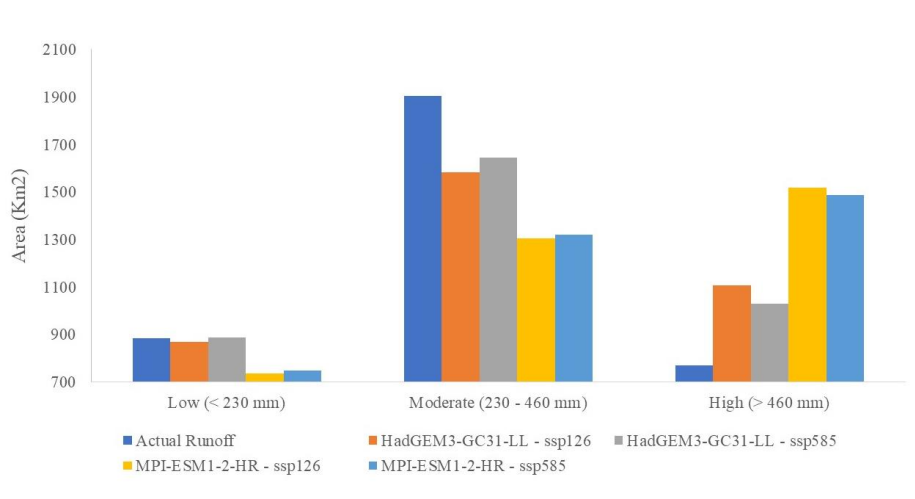

Figure 10: Changes in the spatial variation of current surface runoff area concerning climate change scenarios

The analysis of current surface runoff compared to climate change scenarios, Figure 10, reveals significant variations in the spatial distribution of the affected area. In the current scenario, the low runoff category (< 230 mm) covers 884 km², while in future scenarios, this value varies between 736.8 km² and 886.5 km² depending on the climate model. The moderate runoff category (230 - 460 mm) currently covers 1906 km², but under the SSP126 and SSP585 scenarios, this area is reduced to 1305.5 km² and 1644.3 km². Notably, the high runoff category (> 460 mm) experiences a significant increase under the future scenarios, from 770 km² today to a range between 1029.3 km² and 1517.8 km². Sustainable water resource management may be jeopardized by the increased frequency and intensity of extreme precipitation events suggested by this rise in high runoff areas. These events may also worsen issues with flooding, soil erosion, and surface water availability).

5. Analysis and Discussion

The Huancané River basin's water resource management faces considerable variability and difficulties, as evidenced by the analysis of surface runoff under present and future climatic scenarios. The areas of 884 km², 1906 km², and 770 km² are assigned to the low (<230 mm), moderate (230-460 mm), and high (>460 mm) categories of current runoff, respectively. Low runoff regions shrink marginally to 869.3 km² under the SSP126 scenario, whereas high runoff areas increase to 1107.8 km². High runoff areas rise dramatically to 1517.8 km² under the more extreme SSP585 scenario, suggesting a possible shift toward more intense runoff episodes. The variability in precipitation under the SSP126 and SSP585 scenarios indicates an increasing tendency in both the frequency and severity of rainfall events, with considerable increases at stations such as Ananea and Moho, suggesting a tendency toward increased rainfall event frequency and intensity under the SSP126 and SSP585 scenarios. These findings align with global projections that indicate a warming climate will amplify extreme hydrological events, leading to more significant challenges in water resource management. Changes in soil permeability and land cover further complicate this; higher precipitation rates may cause increased runoff even in regions with lower *CN* values, which indicate higher permeability. These results are supported by studies like [40] and [41], highlighting the vital necessity of adaptive water management techniques.

Dealing with rising flood threats, possible soil erosion, and problems with water quality brought on by more regular high runoff events are among the difficulties of the future. Flood-prone areas identified in this study highlight the need for strategic interventions, such as constructing detention basins, restoring natural floodplains, and reinforcing riparian zones, to minimize the adverse effects of excessive runoff. Reducing the impact of climate variability on hydrological dynamics requires constant monitoring, sustainably managed land use practices, and GIS-based modeling [42] and [43]. Estimating surface runoff is a challenging problem for all academics. It is essential to give the correct *CN* value to each land use and soil feature to evaluate regional runoff. Even though it can be challenging to estimate runoff precisely in broad river basins, improving the outcome [44]. These improvements would reduce uncertainties in runoff predictions and aid in developing localized water management strategies critical for regions like the Huancané River Basin.

6. Conclusions

The amount of surface runoff in the Huancané River basin varies depending on the soil cover and permeability. Areas with dense vegetation and permeable soils have lower runoff values. In contrast, regions with impermeable soils and high slopes have the highest runoff values, particularly in crop and open vegetation areas. It indicates that the physical characteristics of the watershed significantly influence runoff patterns. Therefore, proper land use management is essential for mitigating the risk of erosion and soil loss.

Additionally, all weather stations showed a significant increase in precipitation compared to the scenarios resulting from climate change. It highlights the critical role of watershed physical characteristics in shaping runoff patterns. Sustainable land use practices and soil conservation measures are essential to mitigate erosion and soil loss risks, particularly in vulnerable areas. Climate change projections under scenarios ssp126 and ssp585 reveal a marked increase in precipitation and surface runoff, underscoring the urgency for adaptive water resource management. Historical data (1956–2009) indicates significant precipitation increases at all weather stations. For example, under the ssp585 scenario, the Ananea station, with an average precipitation of 621.7 mm, is projected to rise to 931 mm. These changes will likely amplify flooding and soil erosion risks, particularly in regions with steep slopes and impermeable soils.

The climate change scenarios (ssp126 and ssp585) indicate increased precipitation and surface runoff. According to the HadGEM3-GC31-LL and MPI-ESM1-2-HR models, the areas with the most significant runoff increases are in the lower part of the basin, where runoff can reach values greater than 460 mm, affecting 1107.8 km² in the ssp126 scenario and 1029.3 km² in the ssp585 scenario. Conversely, moderate runoff increases in the upper basin where soils are more permeable, which could lead to saturation and exacerbate landslide risks. These findings emphasize the necessity of tailored watershed management approaches that account for local topography, soil characteristics, and projected climatic shifts. Finally, we recommend investigating the long-term effects of land use changes and soil degradation on runoff patterns and watershed resilience under varying climate change scenarios. Develop adaptive management strategies integrating GIS-based tools to mitigate flood risks and optimize water resource use in the basin.

References

[1] Bal, M., Dandpat, A. K. and Naik, B., (2021). Hydrological Modelling with Respect to Impact of Land-Use and Land-Cover Change on the Runoff Dynamics in Budhabalanga River Basin Using ArcGIS and SWAT Model. *Remote Sensing Applications*, Vol. 23. https://doi.org/10.1016/J.RSASE.2021.100527.

[2] Yang, Y., Weng, B., Man, Z. and Li, C., (2020). Analyzing the Contributions of Climate Change and Human Activities on Runoff in the Northeast Tibet Plateau. *Journal of Hydrology: Regional Studies*, Vol. 27. https://doi.org/10.1016/J.EJRH.2019.100639.

[3] Chagas, V. B. P., Chaffe, P. L. B. and Blöschl, G., (2022). Climate and Land Management Accelerate the Brazilian Water Cycle. *Nature Communications*, Vol. 13, 1-10. https://doi.org/10.1038/S41467-022-32580-X.

[4] Sarkar, T., Kannaujiya, S., Taloor, A. K. and Gupta, S. K., (2020). Integrated Study of GRACE Data Derived Interannual Groundwater Storage Variability Over Water-Stressed Indian Regions. *Groundwater for Sustainable Development*, Vol. 10. https://doi.org/10.1016/J.GSD.2020.100376.

[5] Singh, A. K., Jasrotia, A. S., Taloor, A. K. and Jaiswal, V., (2017). Estimation of Quantitative Measures of Total Water Storage Variation from GRACE and GLDAS-NOAH Satellites Using Geospatial Technology. *Quaternary International*, Vol. 444, 191-200. https://doi.org/10.1016/J.QUAINT.2017.04.014.

[6] Kaliraj, S., Chandrasekar, N., Ramachandran, K. K. and Lalitha, M., (2023). GIS-Based NRCS-CN Modelling of Rainfall-Runoff in River Thamirabarani Sub-Basin, Southern India. *Journal of Hydro-Environment Research*, Vol. 49, 10-27. https://doi.org/10.1016/J.JHER.2023.07.001.

[7] Rajbanshi, J., (2016). Estimation of Runoff Depth and Volume Using NRCS-CN Method in Konar Catchment (Jharkhand, India). *Journal of Civil & Environmental Engineering*, Vol. 6(3), 1-8. https://doi.org/10.4172/2165-784X.1000236.

[8] Smithers, J. C., (2012). Methods for Design Flood Estimation in South Africa. *Water SA*, Vol. 38(5), 633-646.

[9] Wu, S., Chui, T. F. M. and Chen, L., (2021). Modelling Slope Rainfall-Infiltration-Runoff Process with Shallow Water Table During Complex Rainfall Patterns. *Journal of Hydrology*, Vol. 599. https://doi.org/10.1016/J.JHYDROL.2021.126458.

[10] Wang, X., Liu, T. and Yang, W., (2012). Development of a Robust Runoff-Prediction Model by Fusing the Rational Equation and a Modified SCS-CN Method. *Hydrological Sciences Journal*, Vol. 57(6), 1118-1140. https://doi.org/10.1080/02626667.2012.701305

[11] Govindaraju, T., Vinutha, T. Y., Rakesh, C. J. and Bheemappa, A., (2024). Surface Runoff Estimation Using SCS-CN Method for Kurumballi Sub-watershed in Shivamogga District, Karnataka, India. *Nature Environment and Pollution Technology*. Vol. 23(2), 843–854. https://doi.org/10.46488/nept.2024.v23i02.020

[12] Banasik, K., Krajewski, A., Sikorska, A. and Hejduk, L., (2014). Curve Number Estimation for a Small Urban Catchment from Recorded Rainfall-Runoff Events. *Archives of Environmental Protection*, Vol. 40(3), 45-54. https://doi.org/10.2478/aep-2014-0032.

[13] Munna, G. M., Alam, M. J., Uddin, M. M. and Shams, S., (2021). Runoff Prediction of Surma Basin by Curve Number (CN) Method Using ArcGIS and HEC-RAS. *Environmental and Sustainability Indicators*. Vol. 11. https://doi.org/10.1016/j.indic.2021.100129.

[14] Ngo, A., Grivel, S., Nguyen, T., and Nguyen, T. (2023). Impact Assessment of Land Use and Land Cover Change on the Runoff Changes on the Historical Flood Events in the Laigiang River Basin of the South Central Coast Vietnam. *International Journal of Geoinformatics*, Vol. 19(10), 51–63. https://doi.org/10.52939/ijg.v19i9.2881

[15] Mahmoud, S. H., (2014). Investigation of Rainfall–Runoff Modeling for Egypt by Using Remote Sensing and GIS Integration. *Catena*, Vol. 120, 111–121. https://doi.org/10.1016/j.catena.2014.04.011.

[16] Mu, W., Yu, F., Li, C. and Yang, T., (2015). Effects of Rainfall Intensity and Slope Gradient on Runoff and Soil Moisture Content on Different Growing Stages of Spring Maize. *Water (Switzerland)*, Vol. 7(6), 2990–3008. https://doi.org/10.3390/w7062990.

[17] Cheng, Q., Ko, C., Yuan, Y. and Zhang, H., (2006). GIS Modeling for Predicting River Runoff Volume in Ungauged Drainages in the Greater Toronto Area, Canada. *Computers and Geosciences*, Vol. 32(8), 1108–1119. https://doi.org/10.1016/j.cageo.2006.02.005.

[18] Ko, C. and Cheng, Q., (2004). GIS Spatial Modeling of River Flow and Precipitation in the Oak Ridges Moraine Area, Ontario. *Computers and Geosciences*, Vol. 30(4), 379–389. https://doi.org/10.1016/j.cageo.2003.06.002.

[19] Sherman, L. K., (1932). On Runoff. *Eos, Transactions American Geophysical Union*, Vol. 13(1), 298–298. https://doi.org/10.1029/tr013i001p00298-1.

[20] Mahmoud, S. H., Mohammad, F. S. and Alazba, A. A., (2014). Determination of Potential Runoff Coefficient for Al-Baha Region, Saudi Arabia Using GIS. *Arabian Journal of Geosciences*, Vol. 7(6), 2041–2057. https://doi.org/10.1007/s12517-014-1303-4.

[21] Alshammari, E., Abdul Rahman, A., Ranis, R., Abu Seri, N., and Ahmad, F. (2024). Investigation of Runoff and Flooding in Urban Areas based on Hydrology Models: A Literature Review. *International Journal of Geoinformatics*, Vol. 20(1), 99–119. https://doi.org/10.52939/ijg.v20i1.3033.

[22] Khalil, R. and Khalil, R., (2017). Determination of Potential Runoff Coefficient Using GIS and Remote Sensing. *Journal of Geographic Information System*, Vol. 9(6), 752–762. https://doi.org/10.4236/jgis.2017.96046.

[23] Usman, M., Ndehedehe, C. E., Farah, H. and Manzanas, R., (2021). Impacts of Climate Change on the Streamflow of a Large River Basin in the Australian Tropics Using Optimally Selected Climate Model Outputs. *Journal of Cleaner Production*, Vol. 315. https://doi.org/10.1016/j.jclepro.2021.128091.

[24] Bermúdez, M., Cea, L., Van Uytven, E. and Poortinga, A., (2020). A Robust Method to Update Local River Inundation Maps Using Global Climate Model Output and Weather Typing-Based Statistical Downscaling. *Water Resources Management*, Vol. 34(13), 4345–4362. https://doi.org/10.1007/s11269-020-02673-7.

[25] Zhou, Y., Batelaan, O., Guan, H. and Fenicia, F., (2024). Evaluation of the Contributions of Climate Change and Overgrazing to Runoff in a Typical Grassland Inland River Basin. *Journal of Hydrology: Regional Studies*, Vol. 52. https://doi.org/10.1016/j.ejrh.2024.101725.

[26] Boughton, W. C., (1989). A Rainfall-Runoff Analysis Method for Regional Studies. *Hydrology and Water Resources Symposium*, Vol. 1989(1), 317–323.

[27] Eniyew, S., Meshesha, D. T., Zeleke, G. A. and Wassie, S. B., (2024). Combining Geospatial Information and SCS-CN for Surface Runoff Estimation in Rib Watershed, Upper Blue Nile Basin, Ethiopia. *Geomatics, Natural Hazards and Risk*, Vol. 15. https://doi.org/10.1080/19475705.2024.2338533.

[28] Mishra, S. K. and Singh, V. P., (2003). Soil Conservation Service Curve Number (SCS-CN) Methodology. Vol. 42. https://doi.org/10.1007/978-94-017-0147-1.

[29] Kumari, M., Diksha, Kalita, P. and Mishra, V. N., Choudhary, A. and Abdo, H. G., (2024). Rainfall-Runoff Modelling Using GIS Based SCS-CN Method in Umiam Catchment Region, Meghalaya, India. *Physics and Chemistry of the Earth, Parts A/B/C*, Vol. 135. https://doi.org/10.1016/J.PCE.2024.103634.

[30] Satheeshkumar, S., Venkateswaran, S. and Kannan, R., (2017). Rainfall-Runoff Estimation Using SCS-CN and GIS Approach in the Pappiredipatti Watershed of the Vaniyar Sub Basin, South India. *Computers, Environment and Urban Systems*, Vol. 3, 1-8, https://doi.org/10.1007/s40808-017-0301-4.

[31] Li, J. and Wong, D. W. S., (2010). Effects of DEM Sources on Hydrologic Applications, Computers. *Environment and Urban Systems*, Vol. 34, 251–261. https://doi.org/10.1016/J.COMPENVURBSYS.2009.11.002.

[32] Rocha, J., Duarte, A., Silva, M., Fabres, S., Vasques, J., Revilla-Romero, B. and Quintela, A., (2020). The Importance of High Resolution Digital Elevation Models for Improved Hydrological Simulations of a Mediterranean Forested Catchment. *Remote Sensing (Basel)*, Vol. 12, 1-17. https://doi.org/10.3390/rs12203287.

[33] Kenward, T., Lettenmaier, D. P., Wood, E. F., and Fielding, E., (2000). Effects of Digital Elevation Model Accuracy on Hydrologic Predictions. *Remote Sensing of Environment*, Vol. 74, 432–444. https://doi.org/10.1016/S0034-4257(00)00136-X.

[34] Saxton, K. E. and Rawls, W. J., (2006). Soil Water Characteristic Estimates by Texture and Organic Matter for Hydrologic Solutions. *Soil Science Society of America Journal*, Vol. 70, 1569–1578. https://doi.org/10.2136/SSSAJ2005.0117.

[35] Fick, S. E. and Hijmans, R. J., (2017). WorldClim 2: New 1-km Spatial Resolution Climate Surfaces for Global Land Areas. *International Journal of Climatology*, Vol. 37, 4302–4315. https://doi.org/10.1002/JOC.5086.

[36] Calizaya E, Mejía A, Barboza E, Calizaya F, Corroto F, Salas R, Vásquez H, Turpo E. (2021). Modelling Snowmelt Runoff from Tropical Andean Glaciers under Climate Change Scenarios in the Santa River Sub-Basin (Peru). *Water (Switzerland)*, Vol. 13. https://doi.org/10.3390/w13243535.

[37] Ly, S., Charles, C. and Degré, A., (2011). Geostatistical Interpolation of Daily Rainfall at Catchment Scale: The Use of Several Variogram Models in the Ourthe and Ambleve Catchments, Belgium. *Hydrology and Earth System Sciences*, Vol. 15, 2259–2274. https://doi.org/10.5194/HESS-15-2259-2011.

[38] Chen, T., Ren, L., Yuan, F., Yang, X., Jiang, S., Tang, T., Liu, Y., Zhao, C. and Zhang, L., (2017). Comparison of Spatial Interpolation Schemes for Rainfall Data and Application in Hydrological Modeling. *Water*, Vol. 9. https://doi.org/10.3390/W9050342.

[39] Fung, K. F., Chew, K. S., Huang, Y. F., Ahmed, A. N., Teo, F. Y., Ng, J. L. and Elshafie, A., (2022). Evaluation of Spatial Interpolation Methods and Spatiotemporal Modeling of Rainfall Distribution in Peninsular Malaysia. *Ain Shams Engineering Journal*, Vol. 13. https://doi.org/10.1016/J.ASEJ.2021.09.001.

[40] Ahmed, K., Shahid, S. and Nawaz, N., (2018). Impacts of Climate Variability and Change on Seasonal Drought Characteristics of Pakistan. *Atmospheric Research*, Vol. 214, 364–374. https://doi.org/10.1016/J.ATMOSRES.2018.08.020.

[41] Babar, Z. A., Zhi, X. F. and Fei, G., (2015). Precipitation Assessment of Indian Summer Monsoon Based on CMIP5 Climate Simulations. *Arabian Journal of Geosciences*, Vol. 8, 4379–4392. https://doi.org/10.1007/S12517-014-1518-4.

[42] Haleem, K., Khan, A. U., Ahmad, S., Khan, M., Khan, F. A., Khan, W. and Khan, J., (2022). Hydrological Impacts of Climate and Land-Use Change on Flow Regime Variations in Upper Indus Basin. *Journal of Water and Climate Change*, Vol. 13, 758-770. https://doi.org/10.2166/WCC.2021.238.

[43] Fang, X., Ren, L., Li, Q., Zhu, Q., Shi, P., and Zhu, Y., (2013). Hydrologic Response to Land Use and Land Cover Changes within the Context of Catchment-Scale Spatial Information. *Journal of Hydrologic Engineering*, Vol. 18(11), 1539-1548, https://doi.org/10.1061/(ASCE)HE.1943-5584.0000482.

[44] Kumar, A., Kanga, S., Taloor, A. K., Singh, S. K. and Đurin, B., (2021). Surface Runoff Estimation of Sind River Basin Using Integrated SCS-CN and GIS Techniques. *HydroResearch*, Vol. 4, 61–74. https://doi.org/10.1016/j.hydres.2021.08.001.